Immediate response of the DnaK molecular chaperone system to heat shock

Rahel K. Siegenthaler, John P.A. Grimshaw, Philipp Christen*

Biochemisches Institut der Universität Zürich, Winterthurerstrasse 190, CH-8057 Zürich, Switzerland

Received 9 January 2004; revised 11 February 2004; accepted 11 February 2004

First published online 28 February 2004

Edited by Felix Wieland

Abstract The familiar heat shock response in cells comprises the enhanced expression of molecular chaperones. In recent experiments with the Hsp70 system of *Escherichia coli*, the co-chaperone GrpE has been found to undergo a reversible thermal transition in the physiological temperature range. Here, we tested whether this thermal transition is of functional significance in the complete DnaK/DnaJ/GrpE chaperone system. We found that a mere increase in temperature resulted in a higher fraction of fluorescence-labeled peptides being sequestered by DnaK. This direct adaptation of the DnaK/DnaJ/GrpE chaperone system to heat shock conditions may serve to bridge the time lag of enhanced chaperone expression.

Key words: Molecular chaperone; Hsp70; DnaK; Heat shock response; GrpE; Thermosensor

1. Introduction

Molecular chaperones of the 70-kDa heat shock protein (Hsp70) family are essential for the cell to survive environmental stress including heat shock [1,2]. To prevent protein misfolding and aggregation, the chaperones transiently interact with hydrophobic segments of nascent and denatured proteins in an ATP-driven cycle [3,4]. Binding and hydrolysis of ATP induce conformational changes in the NH_2-terminal ATPase domain [5,6], which are communicated to the COOH-terminal peptide-binding domain [7] and modulate its affinity for substrates. The ATP-liganded T state is characterized by low affinity for substrates and fast rates of binding and release, whereas the ADP-liganded R state shows high affinity for substrates and slow kinetics [8,9]. DnaK, an Hsp70 homolog in *Escherichia coli*, acts in concert with its co-chaperones DnaJ, an Hsp40 homolog, and GrpE [3,10,11]. DnaJ stimulates the hydrolysis of DnaK-bound ATP and converts T-state DnaK into high-affinity R-state DnaK (Fig. 1). GrpE facilitates the ADP/ATP exchange and reconverts the R state to the low-affinity T state. The two co-chaperones DnaJ and GrpE conjointly control the fraction of substrate that is sequestered by high-affinity R-state DnaK. Recently, GrpE has been found to undergo a reversible thermal transition within the physiologically relevant temperature range [12–14], while in DnaK and DnaJ no conformational transitions have been observed in this temperature range [12]. Consistent with the structural data, the rate of the DnaJ-triggered T→R conversion follows an Arrhenius temperature dependence, whereas the rate of the GrpE-dependent R→T conversion increases less and less with increasing temperature and even decreases above 40°C [12]. Stabilizing the long NH_2-terminal helix pair of GrpE by an engineered disulfide bond abolishes the thermal transition in GrpE and reduces the deviation of the ADP/ATP exchange activity of GrpE from an Arrhenius temperature dependence, indicating that the long helix pair acts as the primary thermosensor of the chaperone system [15,16]. The present study with the complete DnaK/DnaJ/GrpE chaperone system shows that the thermal responsiveness of GrpE is of functional significance. A mere increase in temperature results in a shift of DnaK from its low-affinity T state toward its high-affinity R state and thus in a higher fraction of substrate being sequestered by DnaK.

2. Materials and methods

2.1. Materials

DnaK was expressed and purified as described previously [17]. Its concentration was determined photometrically with $\varepsilon_{280} = 14\,500\ M^{-1}\ cm^{-1}$ [18]. Purified DnaK contained less than 0.1 mol nucleotide/mol DnaK [17] and was stored at −80°C. DnaJ and GrpE, prepared as reported previously [19,20], were a gift from Dr. H.-J. Schönfeld, Basel. The stock solutions in 50 mM Tris–HCl, 100 mM NaCl, pH 7.7 were kept at −80°C. Peptide NR (NRLLLTG) was purchased from Chiron, Australia (purity >95%) and peptide p4 (CALLQSRLLS) was synthesized by Dr. S. Klauser in our Institute with an ABI 430A Peptide Synthesizer (Applied Biosystems). ATP-Na_2 (purity >98%) and ADP-Na_2 (purity >90%) were purchased from Fluka, Switzerland, and 6-acryloyl-2-dimethylaminonaphthalene (acrylodan) was from Molecular Probes, Eugene, OR, USA.

2.2. Labeling of peptides with acrylodan

Peptide p4 is a derivative of the prepiece of mitochondrial aspartate aminotransferase [9]; peptide NR is another good DnaK binder [21] which has been co-crystallized with the substrate-binding domain of DnaK [7]. The vinyl group of acrylodan served to attach covalently the environmentally sensitive fluorophore to the α-amino group or the sulfhydryl group of peptide NR or p4, respectively. For labeling, NR and p4 were reacted in *N*,*N*-dimethylformamide with acrylodan at a molar ratio of 1.2 and 0.8, respectively, for 3 h at room temperature. The samples were diluted with water to 10% (v/v) *N*,*N*-dimethylformamide, filtrated (0.2 μm), and purified by reverse-phase high-performance liquid chromatography as reported previously [22]. Molecular mass and purity of the acrylodan-labeled peptides were confirmed by mass spectrometry. The concentrations of the stock solutions in 30%

*Corresponding author. Fax: (41)-1-6355907.
E-mail address: christen@bioc.unizh.ch (P. Christen).

Abbreviations: *a*-NR, acrylodan-labeled peptide NR (NRLLLTG); *a*-p4, acrylodan-labeled peptide p4 (CALLQSRLLS); Hsp70, 70-kDa heat shock protein

0014-5793/04/$30.00
doi:10.1016/S0014-5793(04)00190-5

(v/v) acetonitrile were determined photometrically with $\varepsilon_{380} = 20\,000$ M^{-1} cm^{-1} (Molecular Probes).

2.3. Fluorescence spectra

A Perkin-Elmer spectrofluorimeter LS50B, equipped with a stirrer and a thermostated cuvette holder, was used to record fluorescence emission spectra of *a*-peptides. The solution was heated and cooled at a rate of ~4°C/min. All experiments were performed in assay buffer (25 mM HEPES/NaOH, 100 mM KCl, 10 mM $MgCl_2$, pH 7.0) in a final volume of 800 µl (1×0.4 cm cuvette). Throughout, ADP was added together with inorganic phosphate at the same concentration. The excitation wavelength was set at 370 nm (Raman scattering at 422 nm; bandpass 4 nm) and the spectra were recorded from 400 to 600 nm (bandpass 4 nm) under steady-state conditions.

2.4. Determination of dissociation equilibrium constants

The dissociation equilibrium constants (K_d) of the DnaK·*a*-NR complex in the presence of 1 mM ADP (plus 1 mM inorganic phosphate) or 1 mM ATP were determined by fluorescence titration of peptide *a*-NR (50 nM) with up to 2.5 µM or up to 35 µM DnaK, respectively. A Spex Fluorolog spectrofluorimeter equipped with a stirrer and a thermostated cuvette holder was used. Titration experiments were performed in assay buffer at a starting volume of 800 µl (1×0.4 cm cuvette). The excitation wavelength was set at 370 nm (bandpass 4.6 nm) and emission spectra (bandpass 18.5 nm) were recorded from 400 to 600 nm. Fluorescence intensity and DnaK concentration were linearly corrected for the increased sample volume after addition of DnaK. K_d and ΔF_{max} values were determined from a least-squares fit of the data with the equation

$$\Delta F = PL{\cdot}\Delta F_{max}/P_t = [\Delta F_{max}/(2P_t)][(K_d + L_t + P_t) - ((K_d + L_t + P_t)^2 - 4P_t{\cdot}L_t)^{0.5}]$$

where PL denotes the concentration of DnaK·*a*-NR complex, P_t the total *a*-NR concentration, L_t the total concentration of DnaK and ΔF the difference in fluorescence intensity at 500 nm between *a*-NR in the absence and presence of increasing concentrations of DnaK. Analogous calculations based on the difference in the area between 440 nm and 600 nm gave virtually the same K_d values.

2.5. Fast kinetic measurements

A stopped-flow apparatus (Applied Photophysics SX18 MV) served to record changes in fluorescence of the *a*-peptides upon binding to DnaK. The temperature of the syringes and the cuvette was controlled with a circulating external water bath (±0.5°C). The excitation wavelength was set at 370 nm (bandpass 4.5 nm) and the emitted light passed through a high-pass filter with a 455 nm cut-off. The solutions were equilibrated for at least 5 min at the respective temperature before starting the reaction by mixing volumes of 70 µl each. All experiments were performed in assay buffer. ADP was added together with inorganic phosphate at the same concentration. Reaction traces of at least five measurements were averaged and the reaction rates determined from a double-exponential least-squares fit.

3. Results and discussion

3.1. Calibration of the experimental set-up

The goal of this study was to explore in the complete DnaK/DnaJ/GrpE chaperone system whether an increase in temperature shifts DnaK toward its high-affinity R state. To detect this shift, we used fluorescence-labeled peptides (*a*-peptides, *a* denoting the fluorescent probe acrylodan, see Section 2) as substrates for DnaK. Binding of labeled peptides such as *a*-NR and *a*-p4 to DnaK causes both a blue shift of the emission maximum and an increase in fluorescence emission intensity [9] and thus makes it possible to differentiate the two functional states of DnaK according to their affinity for substrates. Because ADP and ATP compete for the nucleotide-binding site in DnaK, the ADP/ATP concentration ratio determines, in the absence of the co-chaperones, the concentration ratio of ADP-liganded, high-affinity R-state DnaK and ATP-liganded, low-affinity T-state DnaK.

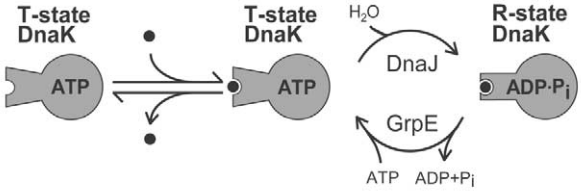

Fig. 1. The DnaK/DnaJ/GrpE chaperone cycle. The substrate is fed into the cycle by fast binding to ATP-liganded T-state DnaK [3,9]. DnaJ-stimulated hydrolysis of DnaK-bound ATP locks DnaK onto the substrate; direct release of substrate from ADP-liganded R-state DnaK is negligibly slow [9]. GrpE-catalyzed ADP/ATP exchange completes the cycle and releases the substrate. The fraction of R-state DnaK, and thus of sequestered substrate, is controlled by the joint action of the co-chaperones DnaJ and GrpE.

To calibrate the experimental set-up, we measured the extent of DnaK·*a*-NR complex formation in the absence of the co-chaperones as a function of the nucleotide concentration ratio (Fig. 2A). Virtually no peptide was expected to bind to ATP-liganded DnaK at the chosen concentrations, because of the low substrate affinity of T-state DnaK (Table 1). The emission spectrum of *a*-NR in the presence of DnaK and ATP was indeed superimposable on the *a*-NR spectrum in the absence of DnaK (not shown). Thus, the blue shift of the emission maximum and the increase in fluorescence intensity with increasing ADP concentration reflect binding of *a*-NR to high-affinity R-state DnaK. The very slow hydrolysis of DnaK-bound ATP does not significantly influence the T state/R state concentration ratio of DnaK because spontaneous ADP/ATP exchange is 10 times faster than hydrolysis [4].

To estimate the fraction of R-state DnaK, i.e. [R state]/([R state]+[T state]), we used either the wavelength of maximum emission (λ^{em}_{max}) or the fluorescence intensity at 500 nm as measured parameter F in the equation $\Delta F/\Delta F'_{max} = (|F - F_0|)/(|F'_{max} - F_0|)$. Values of F_0 and F'_{max} were obtained from the emission spectra in the presence of ATP or ADP, respectively. Thus, $\Delta F/\Delta F'_{max}$ values of 0 and 1 correspond to T-state and R-state DnaK, respectively. In a plot of $\Delta F/\Delta F'_{max}$ versus [ADP]/([ADP]+[ATP]), very similar results were obtained when either λ^{em}_{max} or the fluorescence intensity at 500 nm was used for calculation (Fig. 2B).

For experimentation with the complete DnaK/DnaJ/GrpE chaperone system, the same concentrations of DnaK and peptide were used as above and a DnaJ concentration of 200 nM was chosen according to the physiological DnaK/DnaJ concentration ratio in *E. coli* [23,24]. To determine the concentration range of GrpE in which a change in its ADP/ATP exchange activity would have an observable effect on the fraction of R-state DnaK, we measured the formation of the DnaK·*a*-NR complex at 25°C in the presence of DnaJ, ATP and ADP at varying GrpE concentrations. Because GrpE shifts DnaK toward its T state we used an [ADP]/([ADP]+[ATP]) ratio of 0.8 to start the titration with DnaK being predominantly in the R state. $\Delta F/\Delta F'_{max}$, i.e. the fraction of R-state DnaK, decreased with increasing GrpE concentration reaching a minimum at a concentration of ~50 nM (Fig. 2C). For further experimentation, a GrpE concentration of 40 nM

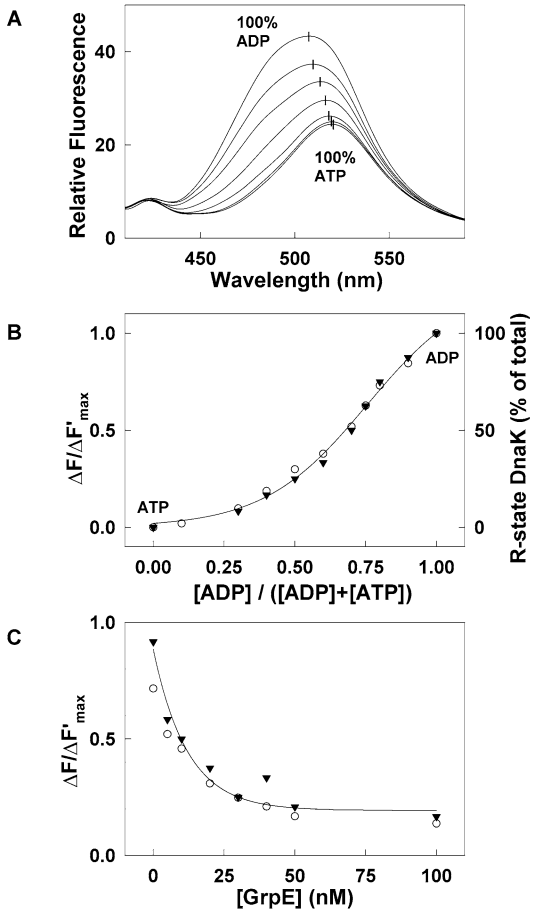

Fig. 2. Calibration of experimental set-up. A: Fluorescence emission spectra (λ_{ex} 370 nm) of 200 nM *a*-NR (final concentrations are indicated throughout), 1 μM DnaK and 1 mM nucleotides (total concentration) were recorded at 25°C at the following [ADP]/([ADP]+[ATP]) ratios: 1 (100% ADP), 0.8, 0.7, 0.5, 0.3, 0.1, 0 (100% ATP). B: $\Delta F/\Delta F'_{max}$ values were calculated on the basis of the fluorescence intensity at 500 nm (○) or λ^{em}_{max} (▼) and plotted versus [ADP]/([ADP]+[ATP]). The solid line represents the best fit to a rectangular hyperbola. C: Plot of $\Delta F/\Delta F'_{max}$ calculated on the basis of the fluorescence intensity at 500 nm (○) or λ^{em}_{max} (▼) versus [GrpE]. Spectra of 200 nM *a*-NR, 1 μM DnaK, 200 nM DnaJ, 1 mM ATP and 4 mM ADP at varying GrpE concentrations at 25°C (not shown) served to calculate the $\Delta F/\Delta F'_{max}$ values. The solid line represents the best fit to a rectangular hyperbola.

was chosen. At this concentration, a temperature-dependent decrease in the nucleotide exchange activity of GrpE was expected to result in an observable shift of DnaK toward its R state, a decrease in exchange activity having the same effect as a decrease in GrpE concentration.

Table 1
Dissociation equilibrium constants of the DnaK·*a*-NR complex at different temperatures

Temperature (°C)	K_d (μM)	
	With ATP	With ADP
25	36	0.38
35	17	0.38
45	14	0.56

The values were determined by fluorescence titration of 50 nM *a*-NR in assay buffer containing 1 mM ATP or ADP with up to 35 μM or up to 2.5 μM DnaK, respectively. Averaged K_d values from two or three measurements are shown.

3.2. *Effect of temperature on the fraction of high-affinity R-state DnaK in the complete DnaK/DnaJ/GrpE chaperone system*

The effect of temperature on the fraction of R-state DnaK was measured at fixed concentrations of DnaK, DnaJ, GrpE, *a*-NR, ATP and ADP. Increasing temperature resulted in a progressive blue shift of λ^{em}_{max} (Fig. 3A), indicating a shift of DnaK toward its high-affinity R state. The fluorescence intensity decreased with increasing temperature due to enhanced collisional quenching [25]. In the control without the co-chaperones (Fig. 3B), the thermal quenching of fluorescence was not compensated in part by increased formation of the DnaK·*a*-NR complex as observed in Fig. 3A. In contrast to the fluorescence intensity at 500 nm, λ^{em}_{max} proved to be temperature-independent. The value of $\Delta F/\Delta F'_{max}$ in the presence

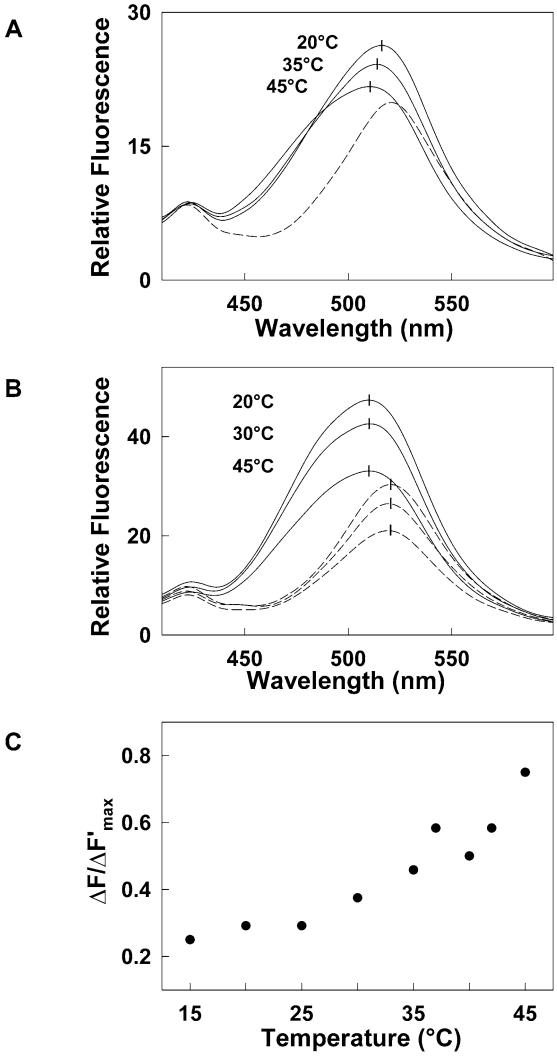

Fig. 3. Formation of the DnaK·*a*-NR complex in the presence of DnaJ and GrpE as a function of temperature. A: Fluorescence emission spectra (λ_{ex} 370 nm) of 200 nM *a*-NR, 1 μM DnaK, 200 nM DnaJ, 40 nM GrpE, 1 mM ATP and 4 mM ADP at the indicated temperatures. The dashed line represents the *a*-NR spectrum in the absence of the chaperone system at 20°C. B: Spectra of 200 nM *a*-NR, 1 μM DnaK and 1 mM ADP at the indicated temperatures. The dashed lines denote *a*-NR spectra in the absence of DnaK. C: Plot of $\Delta F/\Delta F'_{max}$ calculated on the basis of λ^{em}_{max} (from spectra as in A) versus temperature.

of the co-chaperones was therefore calculated with λ^{em}_{max} as measured parameter and plotted as a function of temperature (Fig. 3C). From the $\Delta F/\Delta F'_{max}$ values we conclude that the fraction of R-state (i.e. peptide-liganded) DnaK increased from ~25% of total DnaK at 15°C to ~75% at 45°C. With peptide *a*-p4 as a substrate, similar data were obtained (Fig. 4A–C). Apparently, in the complete DnaK/DnaJ/GrpE chaperone system, a temperature-dependent decrease in the nucleotide exchange activity of GrpE results in a shift of DnaK from its low-affinity T state toward its high-affinity R state.

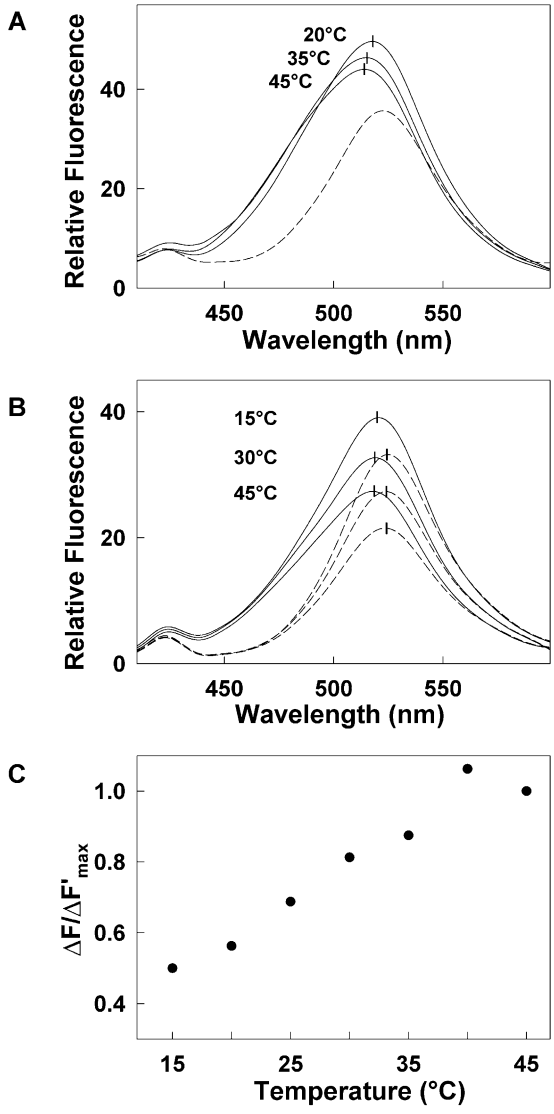

Fig. 4. Formation of the DnaK·*a*-p4 complex in the presence of DnaJ and GrpE as a function of temperature. A: Fluorescence emission spectra (λ_{ex} 370 nm) of 200 nM *a*-p4, 2 μM DnaK, 200 nM DnaJ, 40 nM GrpE, 1 mM ATP and 4 mM ADP at the indicated temperatures. The dashed line represents the *a*-p4 spectrum in the absence of the chaperone system at 20°C. B: Spectra of 200 nM *a*-p4, 2 μM DnaK and 1 mM ADP at the indicated temperatures. The dashed lines denote *a*-p4 spectra in the absence of DnaK. C: Plot of $\Delta F/\Delta F'_{max}$ calculated on the basis of λ^{em}_{max} (from spectra as in A) versus temperature.

3.3. *Effect of temperature on the substrate-binding properties of DnaK in the absence of the co-chaperones*

In the above experiments with the complete chaperone system (Figs. 3 and 4) we determined the fraction of R-state DnaK by the extent of formation of DnaK·*a*-peptide complexes. To confirm that the increased sequestering of peptide at higher temperature is due to the co-chaperones modulating the ATPase cycle rather than to a change in the intrinsic substrate-binding properties of DnaK, we investigated the formation of the DnaK·*a*-peptide complexes in the absence of the co-chaperones at varying temperatures. We found the rates of complex formation with peptides *a*-NR or *a*-p4 to follow an Arrhenius temperature dependence in the presence of ATP or ADP (Fig. 5), indicating that the mechanism of complex formation remains the same from 15°C to 45°C. These findings are consistent with previously reported rate constants of DnaK for fluorescence-labeled Cro peptide between 5°C and 37°C [26]. The dissociation equilibrium constants of the DnaK·*a*-NR complex in the presence of ATP or ADP did not significantly change between 25°C and 45°C (Table 1). Thus, the observed shift of DnaK toward its R state cannot be explained by the temperature dependence of the substrate-binding properties of DnaK itself.

3.4. *Reversibility of the shift of DnaK toward its high-affinity R state*

To examine whether the temperature-induced shift of DnaK toward its high-affinity R state is indeed controlled by the thermosensor action of GrpE [12,13,15,16], we omitted GrpE in the experiment. In the absence of GrpE, the spectra at 15°C and 45°C showed no difference in λ^{em}_{max} (Fig. 6A), indicating that the observed temperature-dependent shift of DnaK toward its R state (Figs. 3A and 4A) depends on the presence of GrpE. The shift toward the R state proved to be fully reversible upon lowering the temperature (Fig. 6B), consistent with the reversibility of the thermal transition of GrpE reported previously [12]. The first and second spectrum at 15°C as well as the two spectra at 45°C were superimposable; the effect of ATP hydrolysis during the experiment appears to be negligible. The functional adaptation of the DnaK system, to both high and low temperature, was found to be already completed within the time period used for attaining the set temperature.

If either ATP or ADP alone was present, no shift of λ^{em}_{max} was observed and the decrease in fluorescence intensity upon increasing temperature was similar to that found in the absence of the co-chaperones (Fig. 6C,D). In the presence of ADP, only R-state DnaK can be formed. In the presence of ATP, DnaK persists predominantly in the T state because under the chosen conditions the GrpE-catalyzed ADP/ATP exchange at both low and high temperature is much faster than the DnaJ-stimulated hydrolysis of ATP, i.e. the T→R conversion.

4. Concluding remarks

The present study shows that temperature directly modulates the functional properties of the DnaK/DnaJ/GrpE chaperone system. A mere increase in temperature suffices to shift DnaK toward its high-affinity R state. This thermal response is due to the divergent temperature dependence of the two co-chaperones. While DnaJ, which stimulates the hydrolysis of

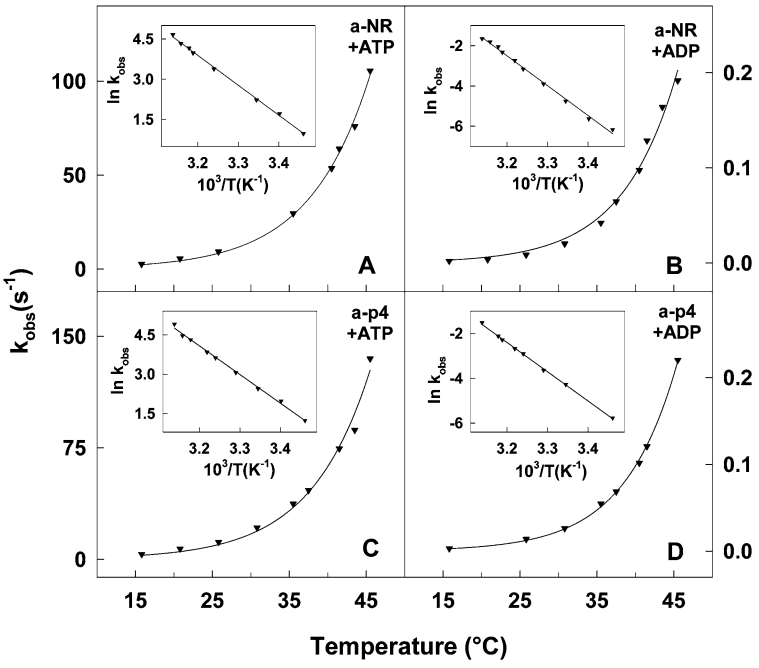

Fig. 5. Rate of formation of DnaK·*a*-peptide complexes as a function of temperature. The following solutions were mixed (final concentrations are indicated): A: [20 μM DnaK, 5 mM ATP]+[500 nM *a*-NR, 5 mM ATP]. B: [20 μM DnaK, 5 mM ADP]+[500 nM *a*-NR, 5 mM ADP]. C: [20 μM DnaK, 5 mM ATP]+[500 nM *a*-p4, 5 mM ATP]. D: [2 μM DnaK, 1 mM ADP]+[200 nM *a*-p4, 1 mM ADP]. Under all conditions, the reactions were biphasic, the rates of both phases showing Arrhenius temperature dependence. The calculated amplitudes of the first and the second phase with peptide *a*-NR were 30% and 70% of total, respectively, in the presence of ADP, and 80% and 20% in the presence of ATP; with peptide *a*-p4 the amplitudes were 15% and 85%, respectively, in the presence of ADP, and 65% and 35% in the presence of ATP. Plots of k_{obs} values of the phase with the higher amplitude versus temperature are shown. The solid lines are Arrhenius curves that have been fitted to the k_{obs} values. Insets show the Arrhenius plots.

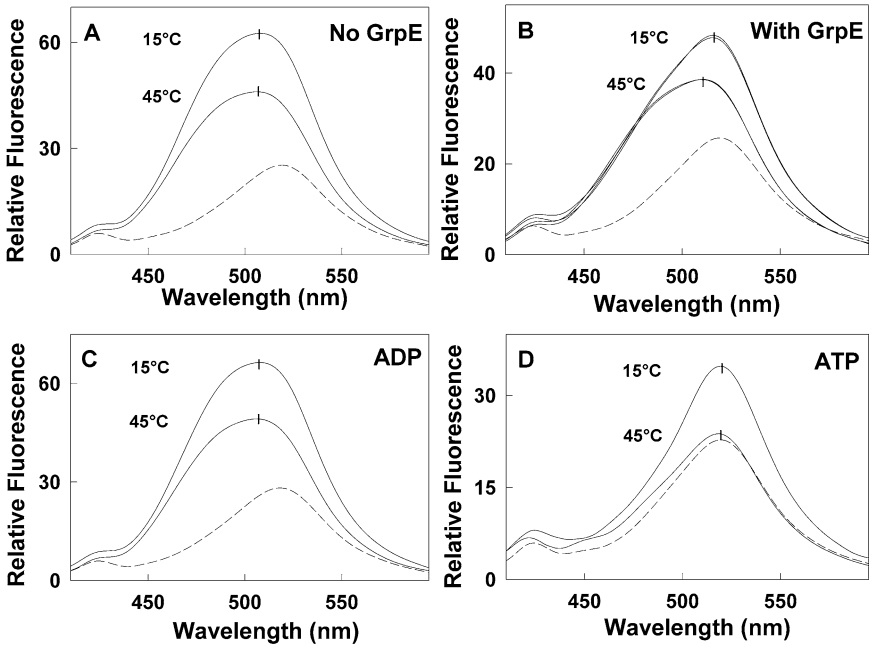

Fig. 6. Formation of the DnaK·*a*-NR complex in the presence and absence of GrpE as a function of temperature. A: Fluorescence emission spectra (λ_{ex} 370 nm) of 200 nM *a*-NR, 1 μM DnaK, 200 nM DnaJ, 1 mM ATP and 4 mM ADP at 15°C and 45°C. The dashed line denotes the *a*-NR spectrum in the absence of chaperones at 45°C. B: Same as A, but in the presence of 40 nM GrpE. The same solution was heated from 15°C to 45°C, cooled to 15°C and reheated to 45°C. C: Spectra of 200 nM *a*-NR, 1 μM DnaK, 200 nM DnaJ, 40 nM GrpE and 4 mM ADP at 15°C and 45°C. The dashed line denotes the *a*-NR spectrum in the absence of chaperones at 45°C. D: Same as C, but in the presence of 1 mM ATP instead of ADP.

DnaK-bound ATP (see Fig. 1), follows an Arrhenius temperature dependence, the ADP/ATP exchange activity of the thermosensor GrpE increases less and less with increasing temperature and even decreases above 40°C [12]. The higher fraction of R-state DnaK increases the fraction of substrate being sequestered by DnaK. We postulate this immediate heat shock response to be relevant to the cell where the ATPase cycle of DnaK also exists in a co-chaperone-controlled steady state [1]. During heat shock, an increase in the fraction of DnaK-bound target protein may be expected to reduce protein aggregation. Mutational analysis in the ATPase domain has indicated that even small disturbances in the ADP/ATP exchange rate suffice to affect the chaperone activity of DnaK [27].

In *E. coli*, the expression level of the DnaK chaperone system is regulated by the alternative sigma factor 32 (σ^{32}), which directs RNA polymerase to transcribe this particular set of genes. Within 5 min after a temperature upshift, the rate of synthesis of the heat shock proteins increases 10–20-fold resulting in an approximately two-fold increase in the cellular concentrations of DnaK, DnaJ and GrpE [2]. The functional adaptation of the extant chaperone system, as reported here, precedes the enhanced expression of its components. The immediate heat shock response might serve to bridge the time lag of the σ^{32}-mediated heat shock response. The instant reversibility upon normalization of temperature might be another important feature of this rapidly deployable protection mechanism. Similar to *E. coli* GrpE, its homolog in the thermophilic bacterium *Thermus thermophilus* has been found to undergo a reversible thermal transition within the physiological temperature range of that organism [13]. The occurrence of a thermosensor action of GrpE in both an archaeon and an eubacterium emphasizes the importance of the immediate heat shock response in prokaryotes.

This study provides unequivocal evidence for the existence of a GrpE-mediated T → R shift of DnaK at heat shock temperatures. Future experiments will have to establish the significance of this mechanistic feature for the chaperone effect on proteins.

Acknowledgements: We thank Antonio Baici and Heinz Gehring for helpful discussions and for critical reading of the manuscript and Hans-Joachim Schönfeld for providing DnaJ and GrpE.

References

[1] Mayer, M.P., Brehmer, D., Gässler, C.S. and Bukau, B. (2001) Adv. Protein Chem. 59, 1–44.
[2] Connolly, L., Takashi, Y. and Gross, C.A (1999) in: Molecular Chaperones and Folding Catalysts (Bukau, B., Ed.), chapter 2, Harwood Academic, Amsterdam.
[3] McCarty, J.S., Buchberger, A., Reinstein, J. and Bukau, B. (1995) J. Mol. Biol. 249, 126–137.
[4] Theyssen, H., Schuster, H.P., Packschies, L., Bukau, B. and Reinstein, J. (1996) J. Mol. Biol. 263, 657–670.
[5] Flaherty, K.M., DeLuca-Flaherty, C. and McKay, D.B. (1990) Nature 346, 623–628.
[6] Harrison, C.J., Hayer-Hartl, M., Di Liberto, M., Hartl, F. and Kuriyan, J. (1997) Science 276, 431–435.
[7] Zhu, X., Zhao, X., Burkholder, W.F., Gragerov, A., Ogata, C.M., Gottesmann, M.E. and Hendrickson, W.A. (1996) Science 272, 1606–1614.
[8] Palleros, D.R., Reid, K.L., Shi, L., Welch, W.J. and Fink, A.L. (1993) Nature 365, 664–666.
[9] Schmid, D., Baici, A., Gehring, H. and Christen, P. (1994) Science 263, 971–973.
[10] Liberek, K., Marszalek, J., Ang, D., Georgopoulos, C. and Zylicz, M. (1991) Proc. Natl. Acad. Sci. USA 88, 2874–2878.
[11] Pierpaoli, E.V., Sandmeier, E., Schönfeld, H.J. and Christen, P. (1998) J. Biol. Chem. 273, 6643–6649.
[12] Grimshaw, J.P.A., Jelesarov, I., Schönfeld, H.J. and Christen, P. (2001) J. Biol. Chem. 276, 6098–6104.
[13] Groemping, Y. and Reinstein, J. (2001) J. Mol. Biol. 314, 167–178.
[14] Gelinas, A.D., Langsetmo, K., Toth, J., Bethoney, K.A., Stafford, W.F. and Harrison, C.J. (2002) J. Mol. Biol. 323, 131–142.
[15] Grimshaw, J.P.A., Jelesarov, I., Siegenthaler, R.K. and Christen, P. (2003) J. Biol. Chem. 278, 19048–19053.
[16] Gelinas, A.D., Toth, J., Bethoney, K.A., Langsetmo, K., Stafford, W.F. and Harrison, C.J. (2003) Biochemistry 42, 9050–9059.
[17] Feifel, B., Sandmeier, E., Schönfeld, H.J. and Christen, P. (1996) Eur. J. Biochem. 237, 318–321.
[18] Hellebust, H., Uhlen, M. and Enfors, S.O. (1990) J. Bacteriol. 172, 5030–5034.
[19] Schönfeld, H.J., Schmidt, D. and Zulauf, M. (1995) Prog. Colloid Polym. Sci. 99, 7–10.
[20] Schönfeld, H.J., Schmidt, D., Schröder, H. and Bukau, B. (1995) J. Biol. Chem. 270, 2183–2189.
[21] Gragerov, A., Zeng, L., Burkholder, W.F. and Gottesman, M.E. (1994) J. Mol. Biol. 235, 848–854.
[22] Pierpaoli, E.V., Sandmeier, E., Baici, A., Schönfeld, H.J., Gisler, S. and Christen, P. (1997) J. Mol. Biol. 269, 757–768.
[23] Bardwell, J.C., Tilly, K., Craig, E., King, J., Zylicz, M. and Georgopoulos, C. (1986) J. Biol. Chem. 261, 1782–1785.
[24] Liu, X. (2002) M.D. Thesis, Universität Zürich.
[25] Pesce, A.J., Rosén, C.G. and Pasby, T.L. (1971) Fluorescence Spectroscopy, Marcel Dekker, New York.
[26] Farr, C.D., Galiano, F.J. and Witt, S.N. (1995) Biochem. 34, 15574–15582.
[27] Brehmer, D., Rüdiger, S., Gässler, C.S., Klostermeier, D., Packschies, L., Reinstein, J., Mayer, M.P. and Bukau, B. (2001) Nat. Struct. Biol. 8, 427–432.